forests

MDPI

Article

Structure Effects on Mechanical Properties of a Novel Engineered Wood Product: Cross-Laminated-Thick Veneers Based on Infinite Splicing Technology

Yuxin Yang [1], Juan Hu [1,2], Xinguang Ning [3], Yahui Zhang [1,*], Yingqi He [1], Yingchun Gong [1], Wenji Yu [1] and Yuxiang Huang [1]

[1] Research Institute of Wood Industry, Chinese Academy of Forestry, Beijing 100091, China; yuxiny@caf.ac.cn (Y.Y.)
[2] Beijing Key Laboratory of Wood Science and Engineering, Beijing Forestry University, Beijing 100083, China
[3] Penglai Zhengtai Wood Industry Co., Ltd., Yantai 265600, China
* Correspondence: zhangyahui@caf.ac.cn

Abstract: With increasing global concern over carbon emissions in the construction industry, cross-laminated-thick veneer (CLTV) has emerged as an innovative green building material with significant potential to promote the achievement of "dual-carbon" goals. This study developed a groove and tenon splicing technique for thick veneers, enabling infinite splicing of the length direction and the preparation of a large-size CLTV measuring 12 m (length) × 3.25 m (width) × 105 mm (thickness). The mechanical properties of CLTV were studied in relation to splice position, assembly pattern of grain directions, and layer combinations. The results showed that increasing the number of // layers (// or ⊥ indicates grain direction of layer parallel or perpendicular to the length direction of CLTV) and using high-level layers significantly improved the compressive strength and reduced the coefficient of variation of CLTV. In terms of bending properties, reasonable splice distribution, placing // layers away from the neutral axis, and elevating layer level dramatically enhanced CLTV performance. Furthermore, the study revealed the synergistic effect among these design elements. The effects of layer level and the number of // layers on mechanical properties varied depending on splice arrangement and assembly pattern of grain directions, highlighting the importance of efficient structural design and raw material selection. This study addresses the limitations of traditional cross-laminated timber in raw material selection and production efficiency. Through structural innovation, it offers a solution for physical design and performance regulation, enabling the application of larger CLTV in wood structures and presenting new ideas for using fast-growing wood to reduce construction emissions.

Keywords: engineered wood product; super-thick wood veneer; alternative low-carbon building materials; cross-laminated-thick veneers; groove and tenon splicing technology; bending properties; compressive strength

Academic Editor: Vasiliki Kamperidou

Received: 24 December 2024
Revised: 10 January 2025
Accepted: 17 January 2025
Published: 19 January 2025

Citation: Yang, Y.; Hu, J.; Ning, X.; Zhang, Y.; He, Y.; Gong, Y.; Yu, W.; Huang, Y. Structure Effects on Mechanical Properties of a Novel Engineered Wood Product: Cross-Laminated-Thick Veneers Based on Infinite Splicing Technology. *Forests* **2025**, *16*, 181. https://doi.org/10.3390/f16010181

1. Introduction

Greenhouse gas emissions are the main factor in global warming and climate change; if not controlled, they will pose a serious threat to human existence [1]. Thereinto, the construction industry accounts for 37% of global greenhouse gas emissions, making it a major contributor to carbon emissions [2,3]. With the implementation of the "dual-carbon" strategy, green building has become essential for the transformation and upgrading of the

construction industry. Substitution of traditional materials with green building materials is crucial for achieving this transformation and meeting the "dual-carbon" goals [4–8]. According to the United Nations Environment Programme (UNEP) and the Yale Center for Ecology and Architecture (Yale CEA), replacing building materials such as cement, steel, and aluminum with renewable, low-carbon, bio-based building materials could reduce industry emissions by up to 40% by 2025 [9]. Among the bio-based, especially wood-based, structural materials, cross-laminated timber (CLT) stands out due to its multi-directional stability [10,11], large size availability, and flexible design [12,13]. CLT is typically composed of three, five, or seven layers of orthogonally arranged wooden boards, with thicknesses ranging from 60 mm to 500 mm and dimensions of 3.5 m in width and up to 16 m in length [14,15]. Researchers utilize the designable properties of CLT structures to achieve higher structural performance or explore feasibility by altering certain design parameters, such as changing the width and thickness of the boards [16], the angle of the transverse layers [17], and the species of wood used for the layers [18]. Researchers are also actively exploring and utilizing CLT's seismic [19–21], fireproof [22,23], and acoustic properties [24,25]. CLT is widely used in modern wood-framed buildings [26], partially replacing reinforced concrete, and brick-concrete structures [27–29]. Aiming to improve mechanical properties, researchers are continuously exploring the blending of materials in the composition of CLT. Wood-based composite materials are used in CLT. In Wang's study, three-layered HCLT made with laminated strand lumber (LSL) or laminated veneer lumber (LVL) as the outer layers effectively improved the bending performance [11,30]. Li's research indicated that oriented strand board is highly suitable as a transverse layer in CLT, and the use of construction oriented strand board (COSB) in CLT can significantly enhance the shear strength and stress. In Wang's experiments, cross-laminated timber-bamboo (CLTB) composed of bamboo scrimber and fir demonstrated the best compressive elastic modulus in axial compression performance testing [31]. However, CLT production still relies on high-quality sawn lumber and large-diameter logs, which are increasingly scarce, limiting the supply of low-carbon raw materials [14,32].

To address this, our project team developed cross-laminated timber veneers (CLTVs) using small-diameter *larch (Larix gmelinii (Rupr.) Kuzen.)*. CLTV matches or exceeds CLT performance at a lower cost [33]. The manufacturing process involves rotary cutting logs into 7.5 mm thick veneers, heat-moisture treatment for stress relief, gluing, assembling, and cold pressing. This method reduces raw material requirements and leverages the CLT structure to overcome the limitations of small-diameter, fast-growing wood. However, current production of CLTV is limited to sizes of 2400 × 1200 mm, which restricts its application in building structures. To expand its use, larger CLTV sizes are needed, achievable through splicing. However, joints can negatively impact overall performance, and inconsistent veneer quality can cause mechanical instability. Therefore, optimizing splicing methods, splice positions, structural design, and layer levels is critical.

CLTV made from different tree species will have varying properties. This study continues previous research by using *larch*, a coniferous species, for designing 19 different types of CLTV to investigate the effects of splice position, grain direction assembly, and layer combinations on mechanical properties under groove and tenon jointing. The goal is to provide structural design and performance regulation solutions for large-size CLTV production, achieving continuous production of one-step-formed large-size CLTV. This will enable the product to be used as a green building material in green construction, providing high-value utilization for small-diameter fast-growing timber. Moreover, using this zero-carbon or even negative-carbon building material to partially replace reinforced concrete, brick-concrete structures, etc., can reduce carbon emissions in the production of building materials, achieving the effect of carbon reduction.

2. Materials and Methods

Larch (Larix gmelinii (Rupr.) Kuzen.) logs with a diameter at breast height of approximately 300 mm were sourced from Hohhot, Inner Mongolia, China. Polyurethane, with a viscosity of about 4500 MPa·s at 25 °C and a pH value of 5–6, was purchased from BASF SE, Shanghai, China.

2.1. Preparation, Classification, and Mechanical Property Evaluation of Larch Thick Veneer

Larch logs were first rotary-cut into 7.5 mm thick veneers with an initial moisture content of 20%. Then, these veneers were subjected to high-temperature pressing to create a hot and humid environment, generating superheated vapors to relieve stress and flatten the veneers. The veneers were classified into three levels based on the rotary cutting position: the part near the heartwood was classified as level 1, with an average density of 0.51 g/cm^3; the outermost part of sapwood was classified as level 3, with an average density of 0.45 g/cm^3; and the middle part between level 1 and level 3 was classified as level 2, with an average density of 0.49 g/cm^3. The static bending strength and modulus of elasticity were tested for each level using the three-point bending method as per GB/T 17657-2022 [34]. Test samples measured 300 × 50 × 7.5 mm, with 50 samples tested per level.

2.2. Preparation of CLTV

Flattened thick veneers were cut into three sizes with grooved and tenoned edges (Figure 1): ① 300 × 300 × 7.5 mm, ② 300 (grain direction) × 150 × 7.5 mm, and ③ 150 (grain direction) × 300 × 7.5 mm. These veneers were assembled into // or ⊥ layers (// or ⊥ indicates grain direction of layer parallel or perpendicular to the length direction of CLTV) to form 600 × 300 mm panels. Five layers were combined with polyurethane glue (300 g/m^2), left to open for 40–50 min, and cold-pressed at 1 MPa for 3 h. Nineteen different CLTV types were produced. A total of 19 different types of CLTVs were prepared in this study for discussion.

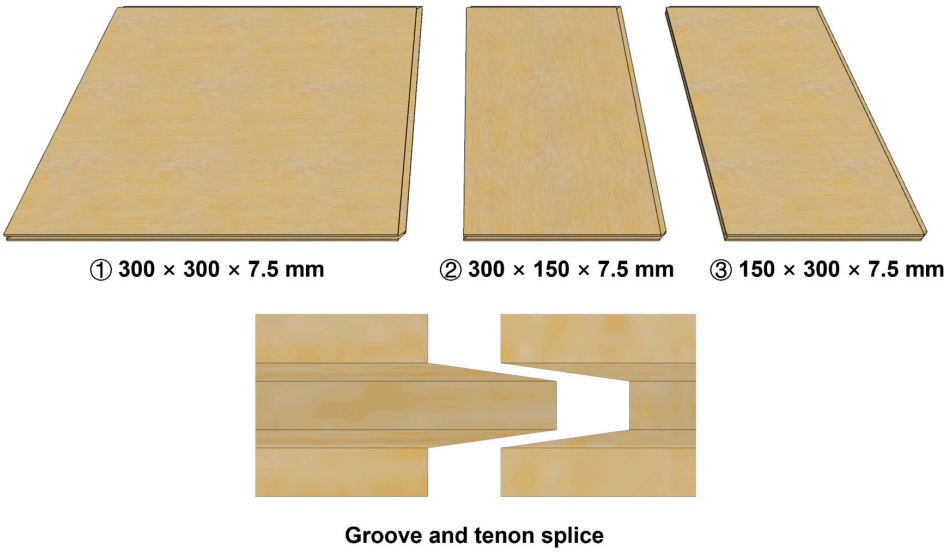

Figure 1. Three sizes of thick veneers with grooved and tenoned edges.

2.2.1. Preparation of CLTV with Different Splice Positions

To investigate the effect of splice position on CLTV performance, CLTVs with different splice positions were prepared using level 1 thick veneers. The veneers were assembled with orthogonal grain directions between adjacent layers, forming two layer orders: surface layer // (//⊥//⊥//) and surface layer⊥ (⊥//⊥//⊥). Two splice locations were used: A, one joint in the center of the layer (spliced by two 300 × 300 mm veneers), and B, two joints 150 mm

from the left and right edges (spliced by one 300 × 300 mm veneer and two 300 × 150 mm or 150 × 300 mm veneers). Five kinds of CLTVs with different splice positions were prepared: BABAB, ABABA, AAAAA, BBABB, and AABAA, as shown in Figure 2.

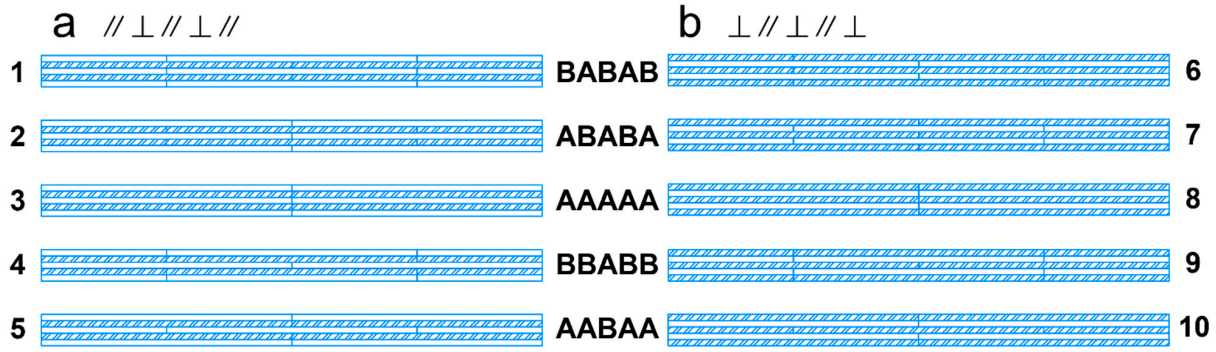

Figure 2. Five splice positions: (**a**) the surface layer is //; (**b**) the surface layer is ⊥.

2.2.2. Preparation of CLTV with Different Assembly Patterns of Grain Directions

To explore the influence of grain direction assembly patterns on CLTV properties, six types of CLTVs were prepared using level 1 veneers and BABAB splice positions. The surface layers were arranged in three // patterns (//⊥⊥⊥//, //⊥//⊥//, // //⊥// //) and three ⊥ patterns (⊥⊥//⊥⊥, ⊥//⊥//⊥, ⊥// //⊥), as illustrated in Figure 3.

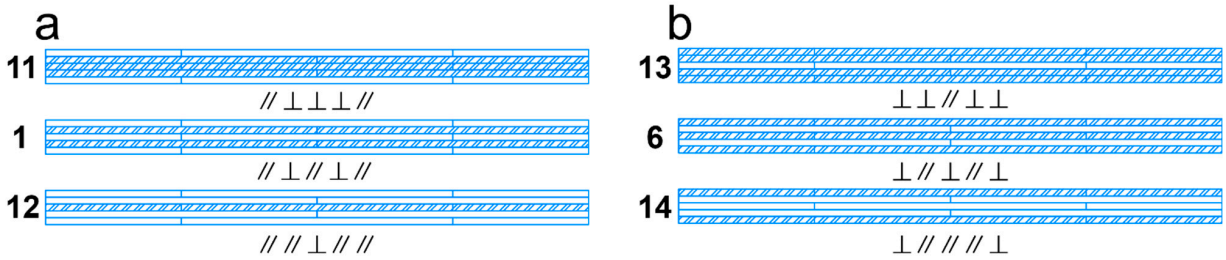

Figure 3. Six assembly patterns of grain directions: (**a**) the surface layer is //; (**b**) the surface layer is ⊥.

2.2.3. Preparation of CLTV with Different Combinations of Layer Levels

To investigate the effect of layer levels on CLTV performance, six types of CLTVs with different layer level combinations were pressed with BABAB splice positions and orthogonal assembly. The surface layers were arranged in // (//⊥//⊥//) and ⊥ (⊥//⊥//⊥) patterns with three combinations: all five layers level 1 (5I), the upper and lower surface layers level 1 and the middle three layers level 3 (3III), and all five layers level 3 (5III) (Figure 4). Additionally, BBABB splice positions were used to compare 5I and 5III with // surface layers.

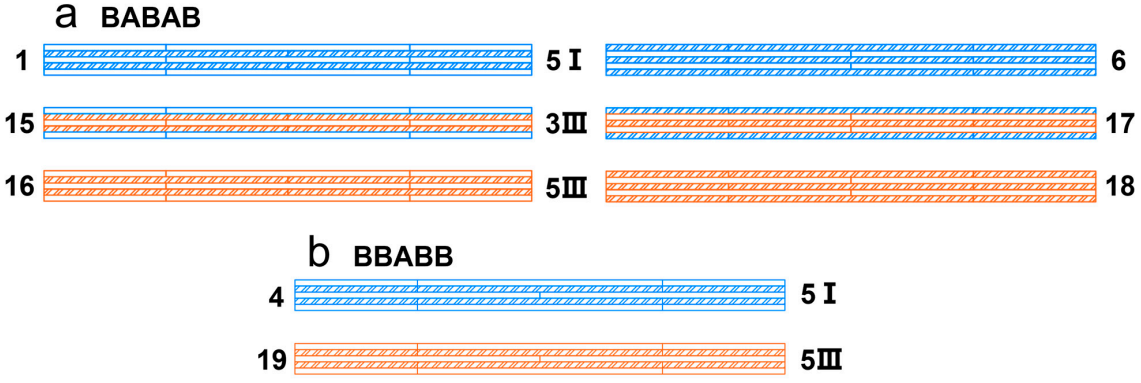

Figure 4. Three combinations of layer levels (Blue represents level 1 layer, and orange represents level 3 layer.): (**a**) splice position BABAB; (**b**) splice position BBABB.

2.2.4. Preparation of Large-Size CLTV

The preparation process of large-size CLTVs is shown in Figure 5. *Larch* logs were rotary cut into 1.2 m × 3.25 m × 7.5 mm veneers and flattened. These thick veneers were then cut into a groove-and-tenon structure. These veneers were then cut into a groove-and-tenon structure along the grain direction. The veneers were connected to form a ⊥ layer measuring 12 m × 3.25 m × 7.5 mm. Square veneers (3.25 m × 3.25 m × 7.5 mm) were also prepared with grooved and tenoned edges and spliced into // layers. The layers were combined with polyurethane glue (300 g/m^2), left to open for 40–50 min, and cold-pressed at 1 MPa for 3 h, resulting in a large-size CLTV measuring 12 m × 3.25 m × 105 mm.

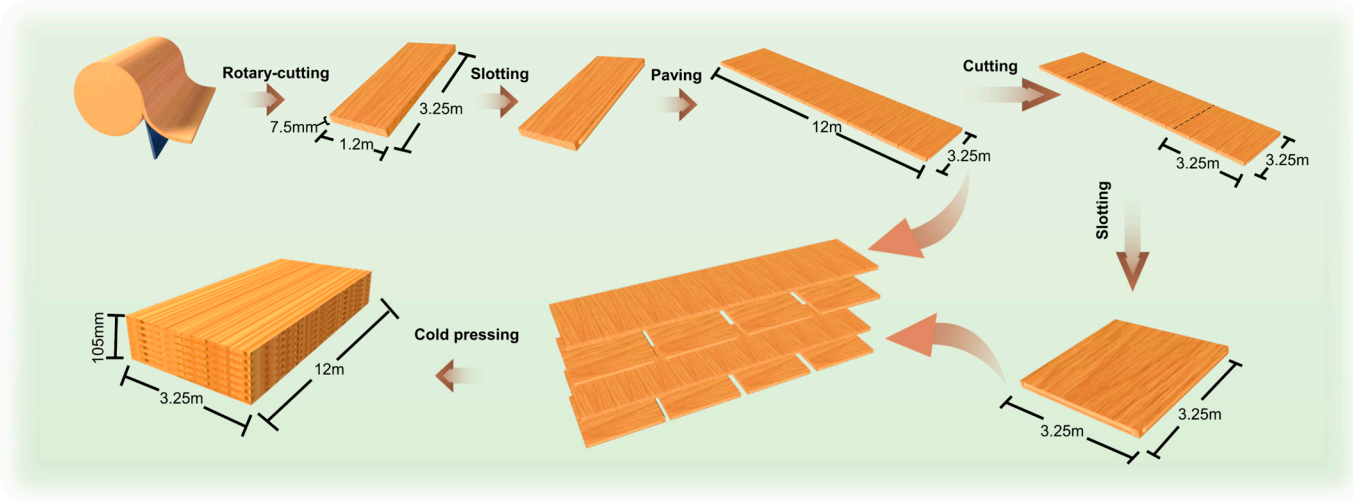

Figure 5. Preparation process of large-size CLTV.

2.3. Compression Test and Bending Test

Compressive strength was measured according to GB/T 1927.11-2022 [35], with specimens sized 35 × 37 × 140 mm. Static flexural strength and modulus of elasticity were tested using the three-point bending method of GB/T 17657-2022 [34], with specimens sized 50 × 37 × 600 mm. Each condition was tested with six samples.

2.4. Statistical Analysis

SPSS (R26.0.0.0) software was used for data analysis in this study. In order to analyze whether there were significant differences among multiple sets of data, the One-way ANOVA Test was used.

2.5. Morphology Observation

The transverse section of different levels of veneer was observed by an ultra-depth-of-field microscope with a magnification of 900.

3. Results and Discussion

3.1. Evaluation of Bending Properties of Different Levels of Thick Veneer

According to the Kolmogorov–Smirnov test results in Table 1, the asymptotic significance values for the flexural strength and modulus of elasticity of level 1, 2, and 3 thick veneers are all greater than 0.05, indicating that the data conform to a normal distribution.

Table 1. Kolmogorov–Smirnov test of different grades of thick veneer.

		Level 1		Level 2		Level 3	
		MOR /MPa	MOE /MPa	MOR /MPa	MOE /MPa	MOR /MPa	MOE /MPa
Number of Cases		50	50	50	50	50	50
Normal Parameters [a,b]	Mean (μ)	75.21	9778.84	62.82	7178.21	53.40	5907.83
	Standard Deviation (σ)	14.76	2344.91	19.42	2231.75	9.31	1087.51
Maximum Difference	Absolute	0.078	0.087	0.104	0.100	0.076	0.116
	Positive	0.049	0.087	0.104	0.100	0.048	0.050
	Negative	−0.078	−0.063	−0.063	−0.073	−0.076	−0.116
Test Statistic		0.078	0.087	0.104	0.100	0.076	0.116
Asymptotic Significance (Two-tailed)		0.200 [c,d]	0.200 [c,d]	0.200 [c,d]	0.200 [c,d]	0.200 [c,d]	0.088 [c]

Note: [a] The test distribution is a normal distribution. [b] Calculated based on the data. [c] Lilliefors significance correction. [d] This is the lower bound of the true significance.

As illustrated in Figure 6, the flexural properties of the three veneer levels follow a normal distribution. The mean (μ) flexural strength values for level 1, 2, and 3 veneers were 75.21 MPa, 62.62 MPa, 53.40 MPa, respectively, and the μ-values of modulus of elasticity (MOE) were 9778.84 MPa, 7178.21 MPa, and 5907.83 MPa, respectively. Level 1 veneers exhibited the highest bending properties, followed by level 2, with level 3 having the lowest. However, the standard deviations (σ) for the flexural strength and elastic modulus of level 2 veneers were relatively high, as could also be seen from flatter curves. This meant that the level 2 data were more dispersed, so that its data range could cover all the level 3 data and most of the level 1 data, which greatly reduced its representativeness. Therefore, only level 1 and level 3 veneers were selected for further study.

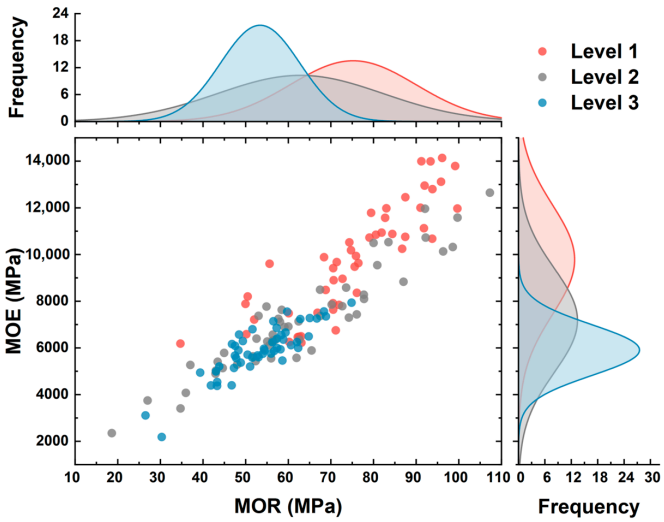

Figure 6. Distribution of bending property of different levels of thick veneer.

3.2. Compressive Strength of CLTV

Table 2 presents the compressive strength results for the 19 CLTVs, showing a trend where compressive strength increases with the number of parallel (//) layers. CLTVs with the same number of // layers exhibited similar compressive strengths, and the compressive strength could be enhanced by increasing the grade of layers. The highest compressive strength, 31.85 MPa, was observed in CLTVs with four // layers, which was 144.73% higher than the compressive strength of 13.01 MPa for CLTVs with only one // layer.

Table 2. Compressive strength of CLTV.

Specimen Number	Compressive Strength			Specimen Number	Compressive Strength		
	Mean /MPa	Standard Deviation /MPa	Variation Coefficient /%		Mean /MPa	Standard Deviation /MPa	Variation Coefficient /%
1	26.67	1.31	4.90	6	20.08	0.65	3.24
2	26.18	1.78	6.81	7	19.07	1.21	6.66
3	26.86	1.19	4.41	8	19.03	0.73	3.85
4	25.70	3.66	14.24	9	21.25	1.82	8.58
5	27.82	1.19	4.27	10	19.82	2.61	11.82
11	20.05	2.02	10.09	13	13.01	0.51	3.94
12	31.85	2.28	7.15	14	28.35	0.68	2.38
15	24.30	1.67	6.89	17	17.52	0.92	5.28
16	24.70	2.55	10.33	18	17.60	1.54	8.77
19	23.41	1.81	7.72				

3.2.1. Effect of Assembly Pattern of Grain Directions on Compressive Strength of CLTV

Since the thickness of the compressive specimens was 140 mm, which was less than the length of 150 mm of types ② and ③ thick veneers in the CLTV axial direction, the specimens only exhibited two splice conditions: no splice and splices located at one end, thus eliminating the influence of the splice position on the compressive strength in the test. Moreover, according to Table S1, the influence of different splice positions on compressive strength is not significant under this cutting size. Therefore, compressive specimens of CLTV with the same grain direction assembly patterns and different splice positions could be classified into one type. At this time, the impact of grain direction assembly patterns on compressive strength was thus attributed to the number of // layers.

When all five layers consisted of level 1 veneers, the compressive strength of CLTV improved with an increase in the number of // layers (Figure 7a,b). The mean values of compressive strength for CLTV with the 1, 2, 3, and 4 // layers were 13.01, 20.11, 26.93, and 31.85 MPa, respectively, This indicates a compressive strength increase of 54.50%, 106.94%, and 144.73% as the number of // layers increased from 1 to 4. Since wood's longitudinal compressive strength is significantly higher than its transverse compressive strength, the ratio of compressive strength of CLTVs with successive numbers of // layers was proportional to the ratio of their // layer counts, aligning with composite laminate theory [36]. For example, the compressive strength ratio for CLTVs with 4 and 3 // layers was 1.18 (close to 1.33), and for those with 3 and 2 // layers, it was 1.34 (close to 1.5). Similar patterns have been observed in other studies [16]. In cases where there are more ⊥ layers or significant differences in their number, the contribution of ⊥ layers to compressive strength cannot be ignored, resulting in notable deviations from these ratios. Although ⊥ layers do not contribute as significantly as // layers in compression tests, having an appropriate number of ⊥ layers can balance the compressive strength along both the strong and weak axes of CLTV. Additionally, the bending deformation caused by ⊥ layers during compression can dissipate energy, evenly distribute pressure, and enhance the stability and overall compressive capacity of the structure. Previous studies have also shown the importance of ⊥ layers in structural applications when their bearing capacity cannot be ignored [31]. The failure modes of the compression specimens are shown in Figure 7c. Under compressive loads, the fibers in the // layers are parallel to the direction of the applied force, playing the primary load-bearing role and thus experiencing greater damage, mainly in the form of fiber buckling, shear slip, and fiber tearing. In contrast, the fibers in the ⊥ layers are perpendicular to the direction of the applied force, bearing less load than the // layers; therefore, the degree of damage is smaller, mainly consisting

of shear damage and bending deformation caused by the failure of the // layers. As the number of // layers increases, the degree of damage to the transverse veneer layers gradually decreases, and the shear failure and crack propagation along the axial direction of the // layers are mitigated. This evolution of the failure mode also confirms the positive correlation between compressive strength and the number of // layers.

Therefore, major changes to the production process are unnecessary; simply rotating the direction of the veneers can yield CLTVs with different compressive properties. In production, the number of // and ⊥ layers in CLTV can be designed according to specific requirements, allowing the manufacture of CLTV that meets various structural needs and fully utilizes the mechanical properties of wood in different directions.

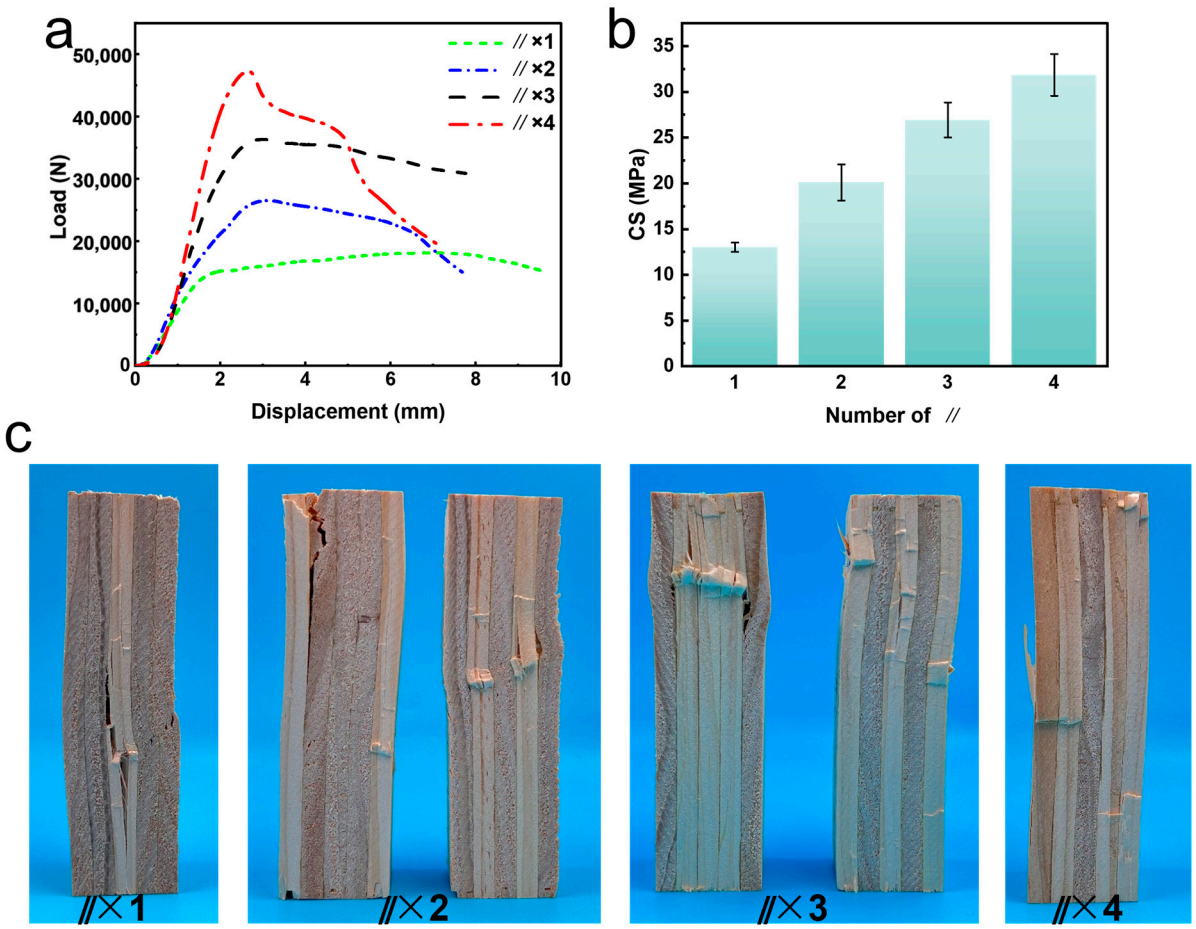

Figure 7. Compressive properties of CLTVs with different numbers of // layers: (**a**) the load–displacement curves; (**b**) compressive strength; (**c**) the failure modes of compressive specimens.

3.2.2. Effect of Combination of Layer Levels on Compressive Strength of CLTV

When both splice positions and grain direction assembly patterns were consistent, CLTV composed entirely of level 1 layers exhibited the highest compressive strength, as shown in Figure 8. The compressive strength of CLTV-5I was 26.67 and 20.08 MPa, which were 7.98% and 14.09% higher than the compressive strength of CLTV-5III, which were 24.7 and 17.60 MPa, respectively. At the same time, with the increase of the number of level 1 layers, the coefficient of variation (CV) in the compressive strength of CLTV observably decreased, as shown in Figure 8c. Moreover, the effect of upgrading the upper and lower surface layers on reducing the CV was greater than that of upgrading the middle layers, which could be reflected by the larger slope. Replacing the upper and lower surface layers of CLTV-5III with level 1 layers to form CLTV-3III did not significantly change the mean compressive strength. However, it decreased the coefficient of variation from

10.33% and 8.77% to 6.89% and 5.28%. The higher coefficient of variation in CLTV-5III diminished the significance of layer level effects on compressive strength in the ANOVA. As shown in Figure 8d, the compression failure modes of CLTV with varying layer level combinations exhibited fiber buckling damage in the // layers. The main differences were observed in the ⊥ layers. When all five layers were level 1, the ⊥ layers suffered the least damage or showed no significant damage. In all other cases, there were noticeable cracks. This indicated that CLTV with higher-level layers has a stronger ability to resist compressive failure. Level 1 veneers derived from the heartwood had a greater density and thicker cell walls compared to level 3 veneers from the sapwood. From the ultra-depth of field microscope images in Figure 9, it can be observed that double-wall thickness of level 1 late-wood cells is significantly thicker, while the difference in cell wall thickness of early-wood cells is not obvious. Therefore, level 1 veneers are more resistant to compressive forces both axially and non-axially, resulting in the highest compressive strength and lowest coefficient of variation of CLTV-5III.

In summary, higher layer levels enhanced compressive performance by increasing compressive strength and reduced coefficient of variation to improve the reliability of the mean performance. Hence, depending on specific requirements, selecting the appropriate combination of layer levels is crucial for optimizing material use in different parts of the wood, which also brings the performance of CLTV closer to the design value.

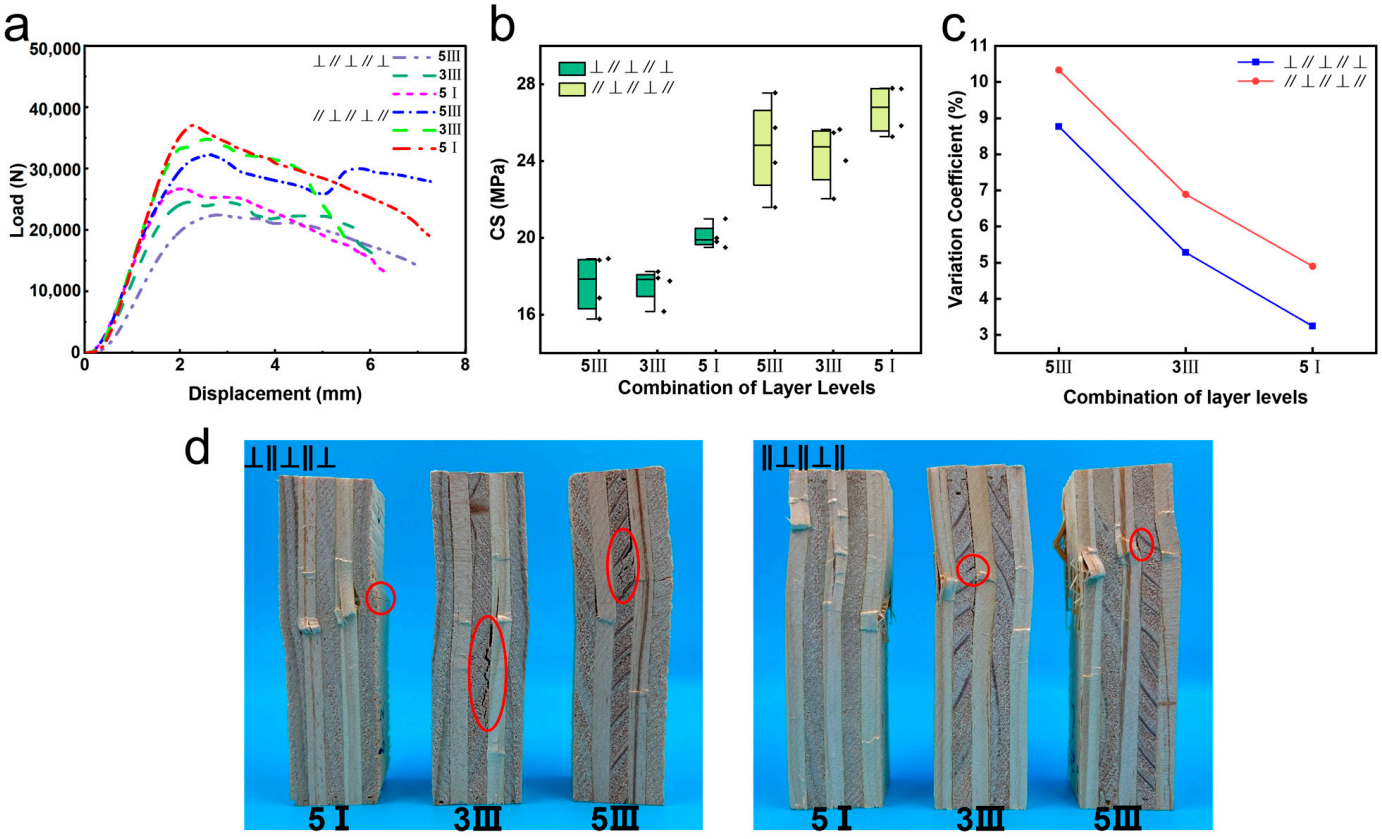

Figure 8. Compressive properties of CLTVs with different combinations of layer levels: (**a**) the load–displacement curves; (**b**) compressive strength; (**c**) variable coefficient; (**d**) the failure modes of compressive specimens (the failure modes of ⊥ layers in red circles).

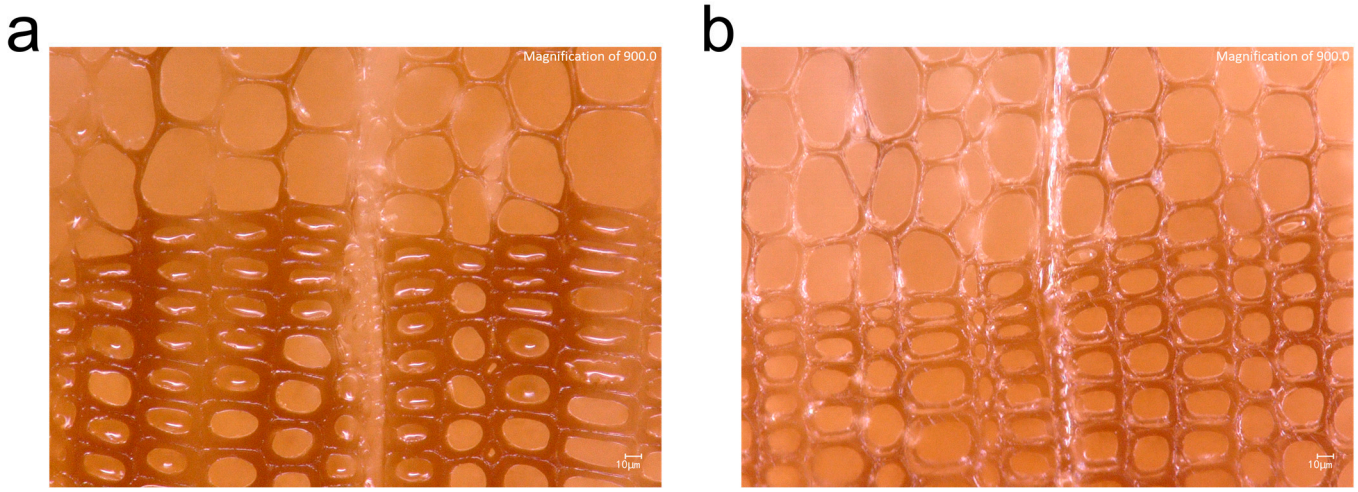

Figure 9. Transverse section of different levels of veneers: (**a**) level 1 veneer; (**b**) level 3 veneer.

3.3. Bending Properties of CLTV

The bending properties of 19 kinds of CLTV were evaluated, and the results are shown in Table 3. The bending strength and modulus of elasticity of the 19 types of CLTV are arranged as shown in Figure 10, generally showing a trend of decreasing bending performance with the reduction of // layers and the decrease in veneer level. At the same time, due to the influence of splice positions, there are arrangements that differ from the overall trend. Notably, CLTVs with four // layers demonstrated the highest MOR and MOE, measuring 38.96 MPa and 7286.31 MPa, respectively. Conversely, CLTVs with three // layers exhibited the lowest MOR at 3.52 MPa, while those with one // layer had the lowest MOE at 478.27 MPa.

Table 3. Bending properties of CLTV.

Specimen Number	MOR		MOE		Specimen Number	MOR		MOE	
	Mean /MPa	STDV /MPa	Mean /MPa	STDV /MPa		Mean /MPa	STDV /MPa	Mean /MPa	STDV /MPa
1	10.16	1.02	5114.79	58.14	6	7.55	1.51	2092.33	67.99
2	3.52	0.66	3178.87	251.65	7	10.47	1.62	1833.73	92.09
3	4.26	0.57	3364.78	658.01	8	7.09	1.19	1960.84	109.68
4	31.20	3.06	5376.79	101.79	9	13.19	2.88	2597.99	124.64
5	21.28	3.27	4162.29	799.44	10	6.94	0.75	1983.68	38.55
11	10.14	1.85	4889.39	53.74	13	5.92	1.01	478.27	7.89
12	38.96	3.09	7286.31	267.24	14	15.28	0.69	2849.27	83.59
15	9.80	0.41	4931.75	304.48	17	5.94	2.40	1771.71	143.03
16	9.61	0.12	4600.25	627.84	18	5.02	0.65	1652.66	179.59
19	14.91	3.19	5152.79	127.81					

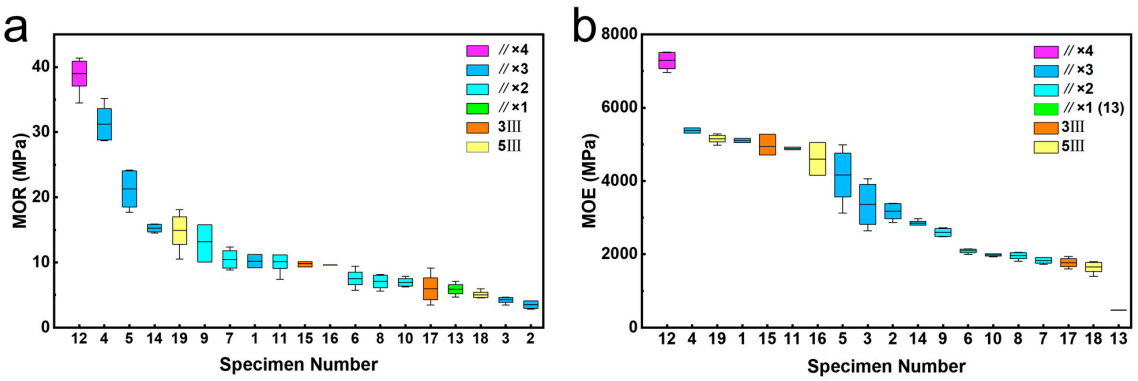

Figure 10. Bending property arrangement trend of the 19 types of CLTV: (**a**) MOR; (**b**) MOE.

3.3.1. Effect of Splice Position on Bending Properties of CLTV

Figure 11 illustrates the bending performance of CLTVs with various splice positions prepared under orthogonal assembly using level 1 layers. Table S3 highlights the significant impact of splice positions on the bending performance of CLTVs. Moreover, the trends in Figures 11a and 12d distinctly show that the bending performance of CLTVs with the same // layer splice positions is similar and is minimally affected by the splice positions in ⊥ layers. Therefore, a further analysis was conducted using variance analysis. Subsequent ANOVA analysis confirmed that under consistent splice positions in // layers, the splice positions in ⊥ layers did not significantly alter the MOR of CLTVs, and except for BB (CLTV7, 9), the splice positions in ⊥ layers also have no significant impact on the MOE of CLTV.

For CLTVs with // surface layers (//⊥//⊥//), those with dispersed // layer splices and surface layer splices on both sides (BAB) displayed superior flexural performance. The MOR and MOE values reached 31.20 MPa and 5376.79 MPa, respectively, surpassing the People's Republic of China Forestry Industry Standard's bending modulus of elasticity value of 5000 MPa for the five-layer assembly form in the TDT9 grade, and significantly exceeding its standard bending strength value of 15.1 MPa. Changing the // layer splice position from a central concentration (AAA) to dispersed distribution with surface layer splices on both sides (BAB) resulted in incremental improvements in MOR: a 161.44% increase from AAA to BBB, followed by a 109.36% increase from BBB to ABA, and finally, a 46.61% increase from ABA to BAB. This is because during the bending test, the outermost veneer layers, which are farther from the neutral axis, generate a greater bending moment and thus are subjected to greater compressive and tensile stresses, contributing more significantly to the overall bending performance. Moreover, below the loading point and near the support points, due to the transmission and distribution of forces, stress concentration occurs. If this exceeds the yield strength of the outer layer material, early local failure may occur. Therefore, distributing the splice positions of the outer layers between the loading point and the support point ensures that continuous and consistent material in the length direction is used where the bending moment is the greatest, allowing it to bear greater stress and thereby enhancing the overall bending properties. Additionally, the bending strength of wood along the grain is much higher than perpendicular to the grain. By dispersing and staggering the splice positions of the neutral axis // layer and the outer // layers, it is possible to avoid a completely discontinuous interface on a certain cross-section, which could lead to stress concentration. The distribution BAB ensures that surface layers farther from the neutral axis bear greater stresses during bending [37], enhancing overall performance. In contrast, MOE showed a different trend: shifting splice positions from BBB to ABA led to an 18.62% decrease. This change occurs because splices moved from the sides to below the loading point, where stress concentrates due to discontinuities in surface material, thereby reducing the material's ability to resist deformation. Combining the analysis with Figure 11b,c, the load–displacement curves of the CLTVs with // layer splices concentrated under the loading point, such as ABABA and AAAAA, show a lower slope in the early stage of the bending test, indicating a weakness in resisting elastic deformation. In contrast, those with joints concentrated on both sides, like BABAB, can quickly reach a higher stress level during the elastic deformation stage, but due to the concentration of splices, they fail rapidly after reaching the yield point, lacking a plastic deformation stage. The CLTV with dispersed splices but with the surface joints under the loading point, AABAA, shows local failure in the early stage. The CLTV with dispersed splices and surface joints on both sides, BBABB, demonstrates a more balanced capability; it can effectively resist elastic deformation in the early stage of bending and can withstand a significant amount of plastic deformation before failure, resulting in higher overall bending

properties. In Lin's research, it is also mentioned that the splices are dispersed away from the loading point to improve the bending performance [38].

When surface layers are ⊥ layers (⊥//⊥//⊥), similar patterns in bending performance due to splice positions were observed. Concentrated splice positions in // layers led to failure concentrated at splices and rapid failure rates. Increased ⊥ layer proportions also intensified the impact of their splice positions, particularly on MOE. For instance, ABABA and BBABB, despite having identical // layer splice positions, showed a 29.42% MOE decrease in ABABA due to concentrated ⊥ layer splices under the loading point.

From the above results, it is evident that splice positions, particularly in // layers, significantly influence CLTV bending performance. Strategically distributing // layer splices effectively mitigates their impact on overall material bending properties, highlighting the potential for scaling up CLTV production through groove and tenon splicing for large-scale applications.

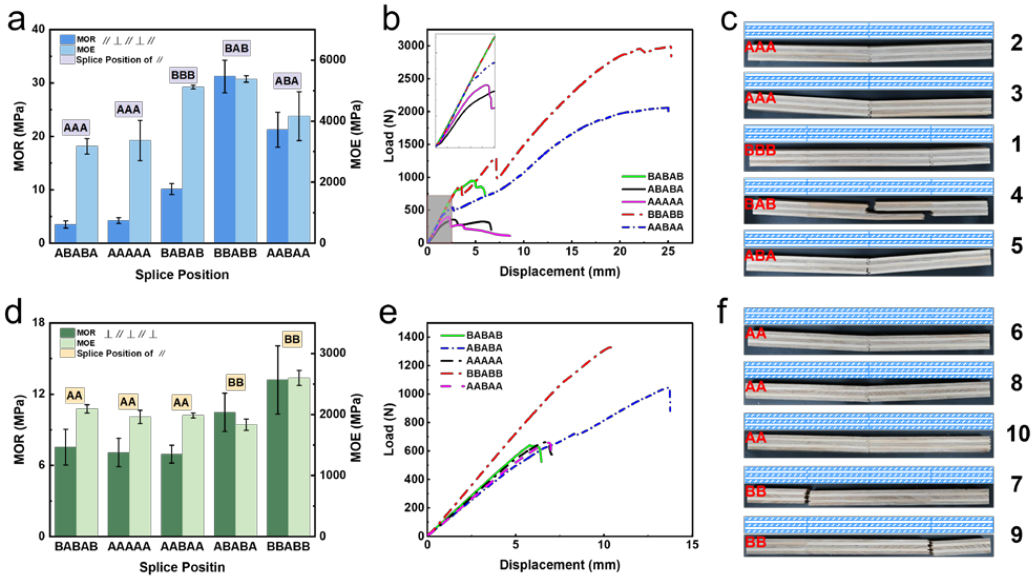

Figure 11. Bending test results of CLTV with different splice positions: (**a**,**d**) bending properties; (**b**,**e**) load–displacement curves; (**c**,**f**) failure modes.

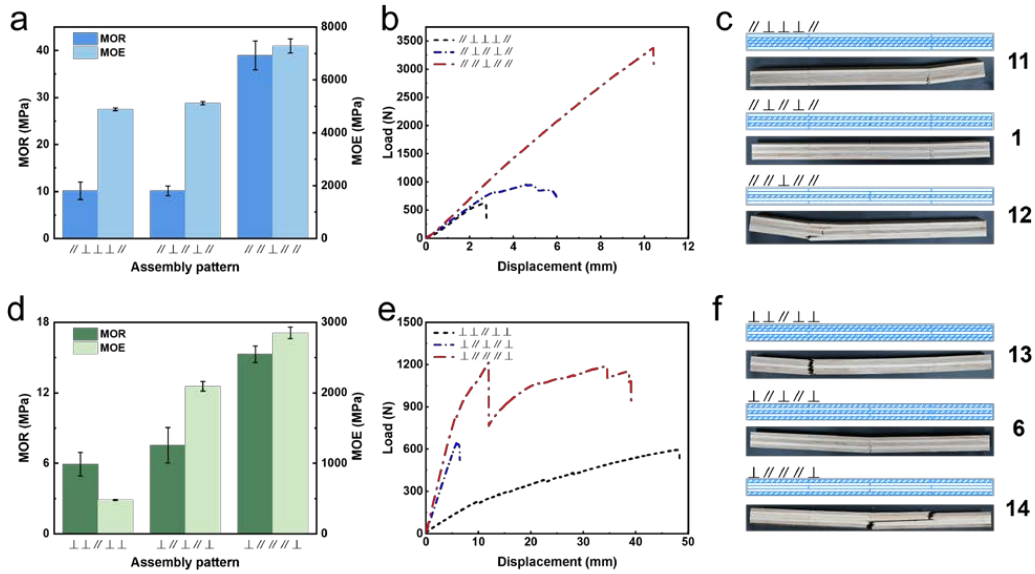

Figure 12. Bending test results of CLTV with different assembly patterns of grain directions (**a**) and (**d**) bending properties; (**b**,**e**) load–displacement curves; (**c**,**f**) failure modes.

3.3.2. Effect of Assembly Pattern of Grain Directions on Bending Properties of CLTV

Figure 12 illustrates the bending properties of CLTVs prepared with different assembly patterns of grain directions, all using level 1 thick veneers and splice position BABAB. Table S4 confirms that the MOR and MOE of CLTVs are extremely significantly affected by the assembly pattern. As can be seen from Figure 12a,d, the bending properties of CLTVs improve notably with an increase in the number of // layers, irrespective of whether the surface layers are oriented as // or ⊥.

Compared to //⊥⊥⊥//, the enhancement in bending performance for //⊥//⊥// is not significant, because merely replacing the neutral layer with a // layer and concentrating the splice positions of the three // layers is insufficient to strongly support the enhancement of CLTV's bending performance. In contrast, // //⊥// // compared to //⊥⊥⊥// shows a significant improvement in bending properties. Except for the neutral layer, all other layers use // layup, and the splice positions are dispersed away from the loading point. This assembly method allows the two additional // layers to be effectively combined with the surface // layers, enabling them to efficiently perform bending resistance where the bending moment is large. The MOR and MOE peak at 38.96 MPa and 7286.31 MPa, respectively, which are increased by 284.33% and 49.02%. Similarly, when the surface layer is ⊥, replacing the outer layers with // layers (⊥⊥//⊥⊥→⊥//⊥//⊥) significantly improves the bending performance. Then, replacing the neutral layer with a // layer whose splice position is different from that of the outer layers (⊥// // //⊥) leads to a remarkable enhancement in bending properties, with MOR increasing to 2.03 times and MOE increasing by 36.18%. Despite this, when comparing CLTV-14 (⊥// // //⊥) with the previously tested CLTV-5 (//⊥//⊥//), although both have the same number and splice positions of // layers, the latter's // layers are located in the outer layers, resulting in superior bending performance, with MOR and MOE being 1.39 and 1.46 times that of the former, respectively.

These findings underscore that the impact of grain direction assembly patterns on CLTV bending properties hinges not only on the quantity of // layers but also, significantly, on the strategic placement of these layers and their splice positions. Thus, regulating mechanical properties of CLTVs can be achieved through deliberate adjustments in grain direction assembly patterns and splice positions.

3.3.3. Effect of Combination of Layer Levels on Bending Properties of CLTV

Figure 13a presents the bending properties of CLTVs prepared with different layer level combinations using an orthogonal assembly pattern with splice positions at BABAB. An increase in level 3 layers shows a slight decrease in bending properties, as evidenced in Table S5, although this trend lacks statistical significance. This marginal effect can be attributed to concentrated splice positions of // layers, which occasionally induce localized material damage, thereby attenuating the impact of veneer levels on CLTV performance.

To further explore these findings, we examined the effect of different layer level combinations on bending properties using the BBABB splice position, known for its minimal impact on bending properties, as depicted in Figure 13b. Layer levels significantly influenced the modulus of rupture (MOR), with a transition from level 1 to level 3 resulting in a 52.22% decrease in MOR, while the change in modulus of elasticity (MOE) was less pronounced. This disparity arises because level 1 thick veneers sourced from heartwood possess higher density and thicker cell walls, endowing CLTVs with greater bending strength compared to level 3 veneers, typically sourced from sapwood [39]. Therefore, CLTV made of higher level layers can obtain higher bending properties, consistent with the results of other studies [10]. Notably, the average MOE differs significantly between level 1 and level 3 veneers, measuring 9778.84 MPa and 5907.83 MPa, respectively. How-

ever, the actual CLTVs achieved lower MOE averages at 5376.79 MPa and 5152.79 MPa, respectively, within the experimental sample size and the range of CLTV structures tested (CLTV-4 to CLTV-19). This suggests that while MOE enhancement is constrained within the tested parameters, practical production scenarios could optimize CLTV dimensions, structural design, splice positioning, and grain direction assembly to significantly boost MOE for diverse application needs.

Based on the analysis of the aforementioned experimental results, it becomes evident that CLTVs represent a holistic integration of multiple interdependent elements. Adjustments in individual elements may encounter limitations in effectively regulating CLTV mechanical properties. Therefore, optimizing performance necessitates coordinated adjustments across various elements to fully exploit raw material capabilities, thereby maximizing resource utilization. Moreover, the adaptability inherent in CLTVs, facilitated by adjustable elements, offers avenues for product diversification and customization, presenting viable strategies for the efficient utilization of wood resources across different applications.

Utilizing thick veneer groove-and-tenon splicing technology, we successfully fabricated a large-scale cross-laminated thick veneer (CLTV) measuring 12 m × 3.25 m × 105 mm, depicted in Figure 14a. This increased size provides CLTV with significant advantages for architectural applications, particularly in direct integration within building structures such as walls, floors, and roofs, as illustrated in Figure 14b. The adoption of this large-size CLTV offers several key benefits in construction practices. Firstly, it minimizes the need for numerous splicing points during assembly, thereby reducing structural seams, enhancing overall construction efficiency, and bolstering structural stability. Secondly, aligning the CLTV dimensions with standard building floor heights (typically 3 m) reduces material cutting and waste, thereby optimizing material utilization. Standardized production of large-sized CLTVs can further unlock their potential as prefabricated components for modular construction, capitalizing on the inherent sustainability and low-carbon attributes of wood materials.

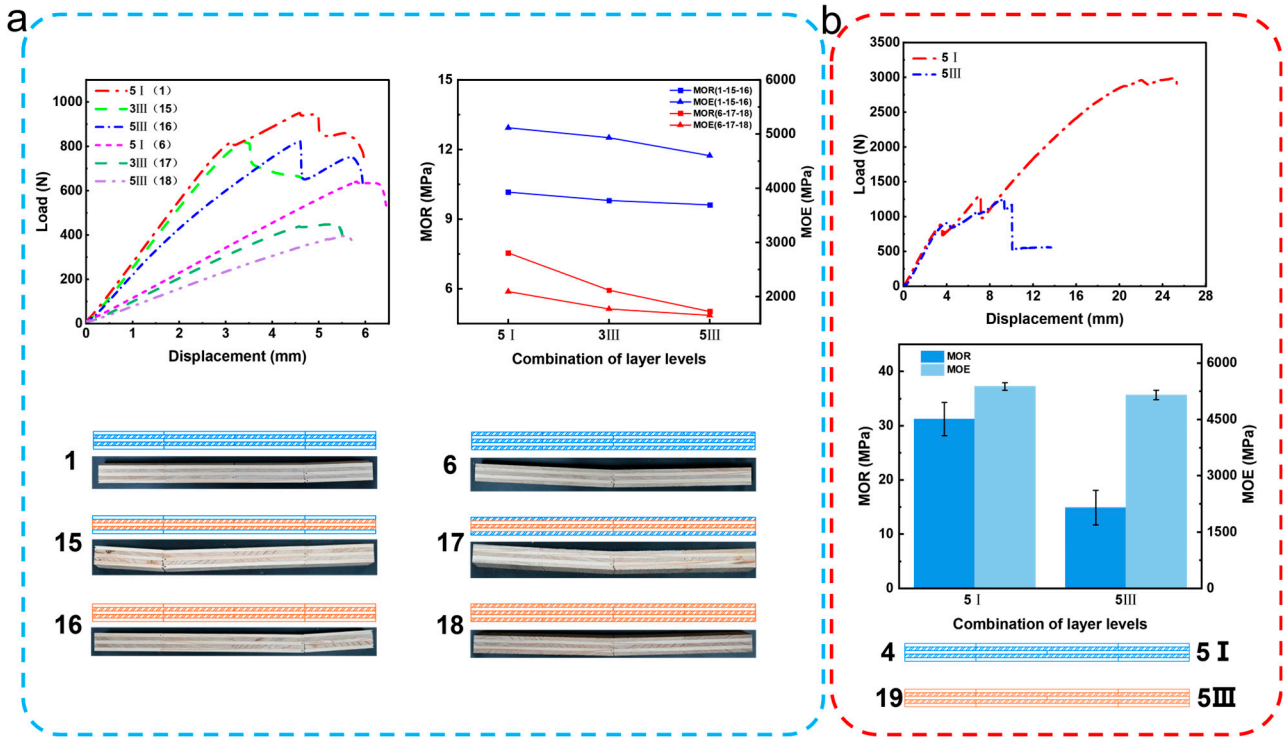

Figure 13. Bending test results of CLTV with different combinations of layer levels: (**a**) splice position BABAB, (**b**) splice position BBABB.

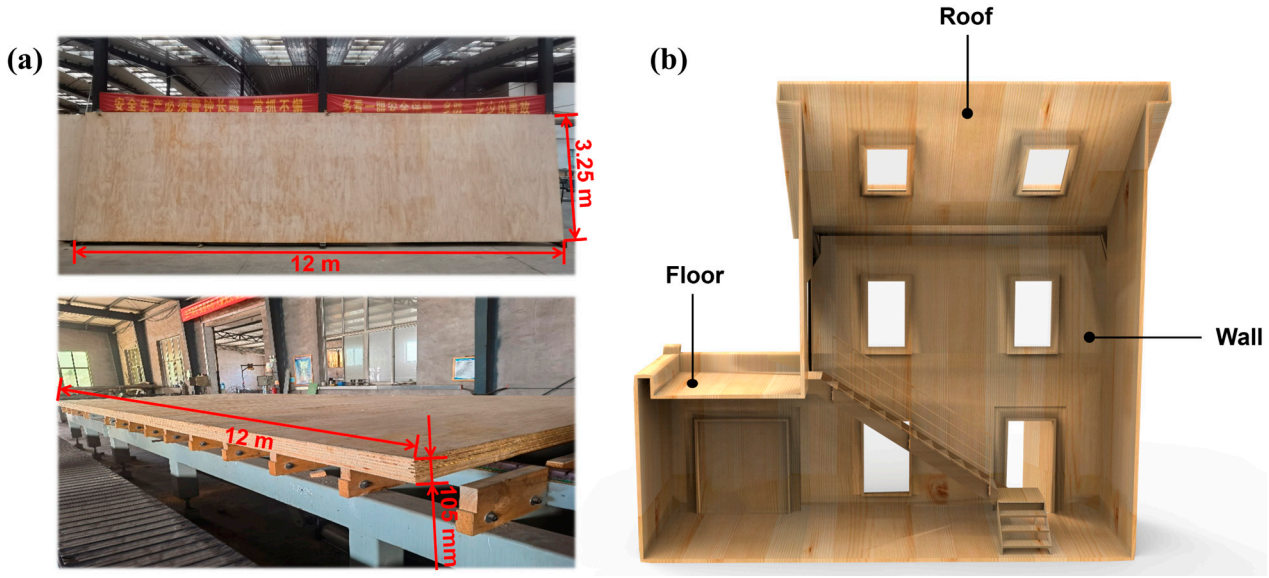

Figure 14. Large-size CLTV in building structures: (**a**) large-size CLTV, (**b**) CLTV cabin effect picture.

4. Conclusions

This study investigated the mechanical properties of cross-laminated-thick veneers (CLTVs) using a groove-and-tenon structure to extend layer splicing. Nineteen variations of CLTVs were analyzed to explore the impacts of splice position, assembly patterns of grain directions, and combinations of layer levels. The results demonstrate that increasing the number of // layers significantly enhances compressive strength by 144.73% in compression tests. Moreover, higher-level veneers improve compression performance by boosting strength and reducing variability. In bending tests, splice positions, layer grain orientations, and layer combinations all exert significant influences on CLTV bending performance. Strategies such as dispersing splices away from load areas, increasing // layer counts, placing // layers on exterior surfaces, and elevating veneer levels positively enhanced bending capabilities. We also found that the effects of these factors on the performance of CLTV are not entirely independent but have synergistic effects. To significantly improve the mechanical properties by upgrading the veneer level or increasing the number of // layers, a rational splice arrangement and effective assembly patterns of grain directions are needed to provide a larger potential for performance improvement, with MOR and MOE potentially increasing by 2.03 times and 1.46 times, respectively. Efficient structural design can capitalize on these elements, showcasing advantages through rational material selection. The findings suggest the feasibility of continuous large-scale production of CLTVs using the groove-and-tenon splicing method. By strategically adjusting splice positions, grain direction assemblies, and layer combinations to meet specific application requirements, CLTVs can be tailored for diverse architectural uses such as roofs, walls, and floors. This approach offers a promising solution for maximizing the utilization of small-diameter timber, addressing global shortages of high-quality wood resources, and promoting wood's role in sustainable construction practices to reduce emissions. At the same time, future research can further explore the proportional relationship between the overall size of CLTV and the splice position, that is, the proportion between the overall size and the basic unit size, so as to improve the entire structural design system of CLTV.

Supplementary Materials: The following supporting information can be downloaded at: https://www.mdpi.com/article/10.3390/f16010181/s1, Table S1: ANOVA of compressive strength of CLTV with different splice positions; Table S2: ANOVA of compressive strength of CLTV; Table S3: ANOVA of bending properties of CLTV with different splice positions; Table S4: ANOVA of

bending properties of CLTV with different assemble patterns of grain direction; Table S5: ANOVA of bending properties of CLTV with different combinations of layer levels.

Author Contributions: Conceptualization, Y.H. (Yuxiang Huang); methodology, Y.H. (Yuxiang Huang); software, Y.Y.; validation, Y.Z.; formal analysis, Y.Y.; investigation, X.N. and Y.G.; resources, W.Y.; data curation, Y.Y.; writing—original draft preparation, Y.Y.; writing—review and editing, Y.Z. and Y.H. (Yuxiang Huang); visualization, Y.Y., J.H. and Y.H. (Yingqi He); supervision, Y.Z. and W.Y.; project administration, W.Y.; funding acquisition, Y.Z. and Y.H. (Yuxiang Huang). All authors have read and agreed to the published version of the manuscript.

Funding: This research was funded by and the Fourth Batch of Forestry and Grassland Science and Technology Innovation Outstanding Young Talent Project, grant number 2024132019, and the Technology-based Small and Medium Enterprises (SMEs) Innovation Capacity Enhancement Project of Shandong Province, grant number 2023TSGC0821.

Data Availability Statement: The original contributions presented in this study are included in the article and Supplementary Materials. Further inquiries can be directed to the corresponding author.

Conflicts of Interest: Author Xinguang Ning was employed by Penglai Zhengtai Wood Industry Co., Ltd. The remaining authors declare that the research was conducted in the absence of any commercial or financial relationships that could be construed as a potential conflict of interest.

References

1. Liu, H.; Yan, N.; Bai, H.; Kwok, R.T.K.; Tang, B.Z. Aggregation-induced emission luminogens for augmented photosynthesis. *Exploration* **2022**, *2*, 20210053. [CrossRef] [PubMed]
2. Ciacci, C.; Banti, N.; Di Naso, V.; Bazzocchi, F. Green strategies for improving urban microclimate and air quality: A case study of an Italian industrial district and facility. *Build. Environ.* **2023**, *244*, 110762. [CrossRef]
3. United Nations. *2022 Global Status Report for Buildings and Construction Towards a Zero-Emissions—Efficient and Resilient Buildings and Construction Sector*; United Nations: New York, NY, USA, 2022.
4. Hildebrandt, J.; Hagemann, N.; Thrän, D. The contribution of wood-based construction materials for leveraging a low carbon building sector in Europe. *Sustain. Cities Soc.* **2017**, *34*, 405–418. [CrossRef]
5. Le, D.L.; Salomone, R.; Nguyen, Q.T. Circular bio-based building materials: A literature review of case studies and sustainability assessment methods. *Build. Environ.* **2023**, *244*, 110774. [CrossRef]
6. Le, D.L.; Salomone, R.; Nguyen, Q.T. Sustainability assessment methods for circular bio-based building materials: A literature review. *J. Environ. Manag.* **2024**, *352*, 120137. [CrossRef]
7. Bourbia, S.; Kazeoui, H.; Belarbi, R. A review on recent research on bio-based building materials and their applications. *Mater. Renew. Sustain. Energy* **2023**, *12*, 117–139. [CrossRef]
8. Li, Y.; Mei, S.; Meng, X.; Qin, Y.; Zhang, P.; Gao, Y. Study on Carbon Emission and Its Reduction Effect of Timber-Concrete Constructions in Xiong'an New District Based on Life Cycle Assessment. *Chin. J. Wood Sci. Technol.* **2022**, *36*, 63–70.
9. United Nations Environment Programme (UNEP); Yale Center for Ecosystems and Architecture (CEA). *Building Materials and The Climate: Constructing a New Future*; United Nations Environment Programme (UNEP): Nairobi, Kenya, 2023.
10. Yin, T.; He, L.; Huang, Q.; Gong, Y.; Wang, Z.; Gong, M. Effect of lamination grade on bending and shear properties of CLT made from fast-growing Chinese fir. *Ind. Crops Prod.* **2024**, *207*, 117741. [CrossRef]
11. Wang, Z.; Gong, M.; Chui, Y.-H. Mechanical properties of laminated strand lumber and hybrid cross-laminated timber. *Constr. Build. Mater.* **2015**, *101*, 622–627. [CrossRef]
12. Stürzenbecher, R.; Hofstetter, K.; Eberhardsteiner, J. Structural design of Cross Laminated Timber (CLT) by advanced plate theories. *Compos. Sci. Technol.* **2010**, *70*, 1368–1379. [CrossRef]
13. Gong, Y.; Ye, Q.; Wu, G.; Ren, H.; Guan, C. Effect of Size on Compressive Strength Parallel to the Grain of Cross-Laminated Timber Made with Domestic Larch. *Chin. J. Wood Sci. Technol.* **2021**, *35*, 42–46.
14. Cherry, R.; Manalo, A.; Karunasena, W.; Stringer, G. Out-of-grade sawn pine: A state-of-the-art review on challenges and new opportunities in cross laminated timber (CLT). *Constr. Build. Mater.* **2019**, *211*, 858–868. [CrossRef]
15. Ido, H.; Nagao, H.; Harada, M.; Kato, H.; Ogiso, J.; Miyatake, A. Effects of the width and lay-up of sugi cross-laminated timber (CLT) on its dynamic and static elastic moduli, and tensile strength. *J. Wood Sci.* **2015**, *62*, 101–108. [CrossRef]
16. He, M.; Sun, X.; Li, Z.; Feng, W. Bending, shear, and compressive properties of three- and five-layer cross-laminated timber fabricated with black spruce. *J. Wood Sci.* **2020**, *66*, 38. [CrossRef]

17. Buck, D.; Wang, X.; Hagman, O.; Gustafsson, A. Bending Properties of Cross Laminated Timber (CLT) with a 45° Alternating Layer Configuration. *Bioresources* **2016**, *11*, 4633–4644. [CrossRef]
18. Aicher, S.; Hirsch, M.; Christian, Z. Hybrid cross-laminated timber plates with beech wood cross-layers. *Constr. Build. Mater.* **2016**, *124*, 1007–1018. [CrossRef]
19. Moroder, D.; Smith, T.; Dunbar, A.; Pampanin, S.; Buchanan, A. Seismic testing of post-tensioned Pres-Lam core walls using cross laminated timber. *Eng. Struct.* **2018**, *167*, 639–654. [CrossRef]
20. Badini, L.; Ott, S.; Aondio, P.; Winter, S. Seismic strengthening of existing RC buildings with external cross-laminated timber (CLT) walls hosting an integrated energetic and architectural renovation. *Bull. Earthq. Eng.* **2022**, *20*, 5963–6006. [CrossRef]
21. Li, Z.; Tsavdaridis, K.D. Design for Seismic Resilient Cross Laminated Timber (CLT) Structures: A Review of Research, Novel Connections, Challenges and Opportunities. *Buildings* **2023**, *13*, 505. [CrossRef]
22. Crielaard, R.; van de Kuilen, J.-W.; Terwel, K.; Ravenshorst, G.; Steenbakkers, P. Self-extinguishment of cross-laminated timber. *Fire Saf. J.* **2019**, *105*, 244–260. [CrossRef]
23. Kleinhenz, M.; Just, A.; Frangi, A. Experimental analysis of cross-laminated timber rib panels at normal temperature and in fire. *Eng. Struct.* **2021**, *246*, 113091. [CrossRef]
24. Di Bella, A.; Mitrovic, M. Acoustic Characteristics of Cross-Laminated Timber Systems. *Sustainability* **2020**, *12*, 5612. [CrossRef]
25. Caniato, M.; Bettarello, F.; Granzotto, N.; Marzi, A.; Gasparella, A. Modelling the impact sound reduction of floating floors applied on cross-laminated timber floors. *J. Build. Eng.* **2024**, *91*, 109679. [CrossRef]
26. O'Ceallaigh, C.; Harte, A.M. The elastic and ductile behaviour of CLT wall-floor connections and the influence of fastener length. *Eng. Struct.* **2019**, *189*, 319–331. [CrossRef]
27. D'Amico, B.; Pomponi, F.; Hart, J. Global potential for material substitution in building construction: The case of cross laminated timber. *J. Clean. Prod.* **2021**, *279*, 123487. [CrossRef]
28. Younis, A.; Dodoo, A. Cross-laminated timber for building construction: A life-cycle-assessment overview. *J. Build. Eng.* **2022**, *52*, 104482. [CrossRef]
29. Zhang, T.T.; Sun, Q.; Sun, X.M.; Shi, J.W.; Ding, Z.P.; Wei, P.X.; Wang, J.H. Research status and localization prospects of cross-laminated timber. *For. Mach. Woodwork. Equip.* **2017**, *45*, 4–7.
30. Wang, Z.; Fu, H.; Gong, M.; Luo, J.; Dong, W.; Wang, T.; Chui, Y.H. Planar shear and bending properties of hybrid CLT fabricated with lumber and LVL. *Constr. Build. Mater.* **2017**, *151*, 172–177. [CrossRef]
31. Wang, Y.; Huang, Q.; Dong, H.; Wang, Z.; Shu, B.; Gong, M. Mechanical behavior of cross-laminated timber-bamboo short columns with different layup configurations under axial compression. *Constr. Build. Mater.* **2024**, *421*, 135695. [CrossRef]
32. Xie, C.; Yue, F.; Yu, H.; Huang, C.; Zeng, S. Evaluation of the stability of droplets in emulsion using multisample analytical centrifugation. *J. Chin. Pharm. Sci.* **2023**, *32*, 574–586.
33. Huang, Y.; Hu, J.; Peng, H.; Chen, J.; Wang, Y.; Zhu, R.; Yu, W.; Zhang, Y. A new type of engineered wood product: Cross-laminated-thick veneers. *Case Stud. Constr. Mater.* **2024**, *20*, e02753. [CrossRef]
34. *GB/T 17657-2022*; Test Methods of Evaluating the Properties of wood-Based Panels and Surface Decorated Wood-Based Panels. Standardization Administration of China: Beijing, China, 2022.
35. *GB/T 1927.11-2022*; Test Methods for Physical and Mechanical Properties of Small Clear Wood Specimens—Part 11: Determination of Ultimate Stress in Compression Parallel to Grain. Standardization Administration of China: Beijing, China, 2022.
36. Pang, S.-J.; Jeong, G.Y. Load sharing and weakest lamina effects on the compressive resistance of cross-laminated timber under in-plane loading. *J. Wood Sci.* **2018**, *64*, 538–550. [CrossRef]
37. Li, H.; Wang, L.; Wei, Y.; Wang, B.J.; Jin, H. Bending and shear performance of cross-laminated timber and glued-laminated timber beams: A comparative investigation. *J. Build. Eng.* **2022**, *45*, 103477. [CrossRef]
38. Lin, Q.; Huang, Y.; Li, X.; Yu, W. Effects of shape, location and quantity of the joint on bending properties of laminated bamboo lumber. *Constr. Build. Mater.* **2020**, *230*, 117023. [CrossRef]
39. Pang, S.-J.; Jeong, G.Y. Effects of combinations of lamina grade and thickness, and span-to-depth ratios on bending properties of cross-laminated timber (CLT) floor. *Constr. Build. Mater.* **2019**, *222*, 142–151. [CrossRef]